Available online at www.sciencedirect.com
SCIENCE DIRECT®
Polyhedron 24 (2005) 881–888
POLYHEDRON
www.elsevier.com/locate/poly

Highly efficient orange-emitting OLEDs based on phosphorescent platinum(II) complexes

Inamur R. Laskar, Shih-Feng Hsu, Teng-Ming Chen *

Department of Applied Chemistry, National Chiao Tung University, Hsinchu, Taiwan

Received 9 November 2004; accepted 4 February 2005
Available online 25 April 2005

Abstract

The syntheses, characterisations, photophysical properties and their applications in organic light emitting devices of a series of 2-phenylbenzothiazolato (bt)/substituted 2-phenylbenzothiazolato (X-bt) platinum(II) based square-planar complexes [(X-bt)Pt(acac); acac = acetylacetonate; X = unsubstituted (**1**), F (**2**), OMe (**3**) and CF_3 (**4**)] are discussed. Reaction of K_2PtCl_4 with btH/X-btH in glacial acetic acid for a few days results in the dinuclear chloro-bridged Pt(II) complex, (bt/X-bt)Pt(μ-Cl)Pt(bt/X-bt) which is cleaved with acetylacetone to give the corresponding mononuclear (bt/X-bt)Pt(acac) complex. The (MeO-bt)Pt(acac) complex has been characterized by X-ray single crystal structure analysis. The packing diagram shows the Pt–Pt distances and the intermolecular spacings are 3.369 and 3.360 Å, respectively, which is consistent with excimer formation. It has also been supported by time-resolved photoluminescence (PL) measurements. The nature of the lowest emitting states are the triplet MLCT as well as triplet π–π* states and it has been tuned according to the electronic properties of the substituents. The electroluminescent (EL) devices were fabricated by doping platinum complexes **1** and **2** (the corresponding devices denoted as D-1 and D-2, respectively) into the host CBP (4,4′-(*N*,*N*′-dicarbazole)biphenyl), in the emitting zone with a doping content of 5%, 7% and 9%. The EL performances for these devices are exceptionally high (14.3 and 16.0 cd A^{-1} @2 mA cm^{-2} and luminances 10 550 and 11 320 cd m^{-2} @100 mA cm^{-2} for D-1 and D-2, respectively).

Keywords: 2-Phenylbenzothiazole; Platinum(II)-complex; Photoluminescence; Eximer; Electroluminescence; Dopant

1. Introduction

The development of organometallic based optoelectronics, such as light-emitting devices, chemosensors and photovoltaic dye-sensitized devices [1] is one of the exciting applications of transition metal complexes. Extensive work on cyclometallating or oligopyridine complexes of Ru(II) [2], Os(II) [3], Re(I) [4] and Ir(III) [5] have been studied for their long triplet excited-state lifetimes, high emission quantum yields and tunable emission wavelengths in the above mentioned areas. Recently, significant research has been focused on the syntheses of cyclometallated complexes of iridium(III) and particularly in light emitting diodes [5]. Platinum(II) complexes have also been used as luminescent centres in organic light-emitting diodes (OLEDs) [6]. Only few of the reported platinum(II) complexes are emissive at room temperature in solution. Pt(II) species chelated with aromatic ligands, such as bipyridine, phenanthroline, 2-phenylpyridine or similar derivatives, emit in solution from excited states localized on the aromatic systems. These Pt(II) complexes benefit from having relatively high metal-centred (MC) states when compared to their palladium analogues [7]. If the emitting states (MLCT or intraligand) and MC states lie too close in energy, they can thermally equilibrate, thereby quenching

* Corresponding author. Tel.: +88635712121x56526; fax: +88635723764.
E-mail address: tmchen@mail.nctu.edu.tw (T.-M. Chen).

0277-5387/$ - see front matter © 2005 Elsevier Ltd. All rights reserved.
doi:10.1016/j.poly.2005.02.009

the emission through fast radiationless decay through the MC states [8]. Moreover, the open coordination centres of the square planar platinum(II) complex can allow for other deactivating pathways to occur through metal interactions with the environment [9]. These facts are responsible for not so encouraging photoluminescence (PL) and electroluminescence (EL) performances of platinum based complexes. Recently, Che et al. reported new orange-yellow emitting schiff-base complexes of platinum(II) [10] showing modest results. The present work reports the syntheses and characterization of some strong orange-emitting cyclometallated platinum(II) complexes, (bt)Pt(acac) (**1**)/(X-bt)Pt(acac) (X = F (**2**), OMe (**3**), CF_3 (**4**); bt = 2-phenylbenzothiazolato; acac = acetylacetonate), study of their photophysical properties, X-ray single crystal structure analysis of (MeO-bt)Pt-(acac) and their applications in OLEDs.

2. Experimental

2.1. Materials

Potassium tetrachloroplatinate(II) was purchased from Alfa Aesar, USA, 2,4-pentanedione from Lanscaster, 2-ethoxyethanol and glacial acetic acid from Tedia Company, Ins. and the rest of the chemicals and solvents (AR grade) from Tokyo Kasei Kogyo Co. Ltd., Japan, and they were used as received.

2.2. Instrumentation

The ultraviolet–visible (UV–Vis) spectra of the phosphorescent Ir(III) complexes were measured on an UV–Vis spectrophotometer (Agilent model 8453) and corrected for background due to solvent absorption. Photoluminescence (PL) spectra were carried out with a spectrofluorometer (Jobin-Yvon Spex, model Fluorolog-3). The photo-physical measurements of these complexes have been carried out in aerated dichloromethane. NMR spectra were recorded on a Varian 300 MHz. MS spectrometer (EI and FAB) were taken by micromass TRIO–2000. Elemental analyses have been carried out by using a Heraeus CHN-O-RAPID analyzer. TG–DTA analysis was carried out by using a thermal analyzer (SEIKO 1TG/DTA 200). Emission lifetimes were obtained by exponential fitting of emission decay curves recorded on a Continuum NY61 spectrofluorometer.

2.3. Crystallography

Single crystal diffraction data for Pt(MeO-bt)(acac) were collected on a Bruker Smart-CCD diffractometer equipped with a normal focus, 3kW sealed-tube X-ray source (λ = 0.71073 Å). The intensity data were collected in the ω scan mode (width of 0.3/° frame) and corrected for *Lp* and absorption effects using the SAINT [11] program. Cell refinement and data reduction were carried out using the program Bruker SHELXTL [12]. The structure was solved by direct methods using the SHELXTL [12] version 5.1 software packages. The structure was further refined by full-matrix least-squares methods based on F^2 using SHELXTL version 5.1 [12]. Non-hydrogen atom positions were refined anisotropically, whereas the hydrogen positions were not refined.

2.4. Syntheses

bt/X-bt (X = –F, –OMe, $–CF_3$): The detailed synthetic procedure of these ligands has been described in the literature [13].

(bt/X-bt)Pt(μ-Cl)$_2$Pt(bt/X-bt) [14]: The ligands (2 mmol) were added to a suspension of potassium tetrachloroplatinate (1 mmol) in glacial acetic acid (300 ml) and the reaction mixture was stirred for several days (3–5 days) whilst maintaining the temperature at ~80 °C, which resulted in a yellow coloured product that was distinctly discernable from the red platinum(II) salt. The product was isolated through filtration and washed with water, acetone and ether 5–6 times to remove almost all the excess starting materials.

(bt)Pt(μ-Cl)$_2$Pt(bt). Yield: 45%. *Anal*. Calc. for $C_{26}H_{16}N_2Cl_2S_2Pt_2$: C, 35.4; H, 1.8; N, 3.2. Found: C, 35.2; H, 1.8; N, 3.1%.

(F-bt)Pt(μ-Cl)$_2$Pt(F-bt). Yield: 48%. *Anal*. Calc. for $C_{26}H_{14}N_2F_2Cl_2S_2Pt_2$: C, 34.0; H, 1.5; N, 3.1. Found: C, 33.7; H, 1.7; N, 3.1%.

(MeO-bt)Pt(μ-Cl)$_2$Pt(MeO-bt). Yield: 50%. ^{1}H NMR (300 MHz, $CDCl_3$): 9.92 (d, 1H, J = 8.7 Hz), 9.93 (d, 1H, J = 7.5 Hz), 8.40 (d, 2H, J = 8.6 Hz), 7.92 (d, 1H, J = 6.3 Hz), 7.78 (d, 1H, J = 6.7 Hz), 7.52 (m, 2H), 7.35 (m, 2H), 6.96 (d, 2H, J = 8.2 Hz), 6.53 (d, 1H, J = 7.2 Hz), 5.56 (s, 1H), 3.81 (s, 3H), 3.51 (s, 3H). *Anal*. Calc. for $C_{28}H_{20}N_2O_2Cl_2S_2Pt_2$: C, 35.4; H, 1.8; N, 3.2. Found: C, 35.2; H, 1.8; N, 3.1%.

(CF_3-bt)Pt(μ-Cl)$_2$Pt(CF_3-bt). Yield: 44%. *Anal*. Calc. for $C_{28}H_{14}N_2F_6Cl_2S_2Pt_2$: C, 33.0; H, 1.4; N, 2.8. Found: C, 32.9; H, 1.4; N, 3.0%.

(bt/X-bt)Pt(acac) [15]: The dinuclear complexes (1 mmol) were dissociated into the mononuclear platinum(II) complexes by reacting with acetylacetone (2.5 mmol) in the presence of sodium carbonate (8 mmol) and 2-ethoxyethanol (10 ml) as solvent under refluxing conditions for 12 h. These complexes show better solubility in common organic solvents with respect to their corresponding dinuclear complexes. These complexes were recrystallised from a mixture of dichloromethane and methanol (1:1).

(bt)Pt(acac): ^{1}H NMR (300 MHz, $CDCl_3$): 9.20 (d, 1H, J = 8.1 Hz), 7.80 (d, 1H, J = 8.1 Hz), 7.69 (d, 1H,

J = 7.5 Hz), 7.47 (m, 3H), 7.19 (d, 1H, J = 7.5 Hz), 7.10 (t, 1H, J = 7.2 Hz), 5.56 (s, 1H), 2.09 (s, 3H), 2.03 (s, 3H). FABMS: *m/z*: 504, Calc. 504.1. *Anal*. Calc. for $C_{18}H_{15}NO_2SPt$: C, 42.8; H, 3.0; N, 2.8. Found: C, 42.5; H, 3.0; N, 2.7%.

(F-bt)Pt(acac): ^{1}H NMR (300 MHz, $CDCl_3$): 9.17 (d, 1H, J = 8.1 Hz), 7.79 (d, 1H, J = 12 Hz), 7.44 (m, 4H), 6.81 (d, 1H, J = 6.0 Hz), 5.78 (s, 1H), 2.10 (s, 3H), 2.04 (s, 3H). FABMS: *m/z*: 522, Calc. 522.1. *Anal*. Calc. for $C_{18}H_{14}NO_2SPt$: C, 41.4; H, 2.7; N, 2.7. Found: C, 42.5; H, 2.6; N, 2.7%.

(MeO-bt)Pt(acac): ^{1}H NMR (300 MHz, $CDCl_3$): 9.11 (d, 1H, J = 8.4 Hz), 7.75 (d, 1H, J = 8.4 Hz), 7.51 (t, 1H, J = 6.7 Hz), 7.39 (m, 2H), 7.19 (d, 1H, J = 2.4 Hz), 6.67 (dd, 1H, J = 2.4, 8.7 Hz), 5.56 (s, 1H), 3.89 (s, 1H), 2.08 (s, 3H), 2.02 (s, 3H). FABMS: *m/z*: 534, Calc. 534.1. *Anal*. Calc. for $C_{19}H_{17}NO_3SPt$: C, 41.4; H, 3.2; N, 2.6. Found: C, 41.2; H, 3.2; N, 2.5%.

(CF_3-bt)Pt(acac): ^{1}H NMR (300 MHz, $CDCl_3$): 9.24 (d, 1H, J = 8.7 Hz), 7.93 (s, 1H), 7.85 (d, 1H, J = 7.2 Hz), 7.52 (m, 3H), 7.34 (d, 1H, J = 7.5 Hz), 5.59 (s, 1H), 2.35 (s, 3H), 2.26 (s, 3H). FABMS: *m/z*: 572, Calc. 572.1. *Anal*. Calc. for $C_{19}H_{14}NO_2F_3SPt$: C, 39.9; H, 2.4; N, 2.4. Found: C, 39.8; H, 2.4; N, 2.4%.

2.5. OLED fabrication and testing

Organic layers were fabricated by high-vacuum thermal evaporation onto a glass substrate precoated with an indium–tin-oxide (ITO) layer with a sheet resistance of 20 Ω. Prior to use, the ITO surface was ultrasonicated in a detergent solution followed by rinsing with deionized (DI) water, dipped into acetone, trichloroethylene and 2-propanol, and then degreased with a vapor of 2-propanol. After degreasing, the substrate was oxidized and cleaned in a UV-ozone chamber before it was loaded into an evaporator. In a vacuum chamber at a pressure of 10^{-6} torr, 500 Å of NPB (*N*,*N*′-di-1-napthyl-*N*,*N*′-diphenylbenzidine) as the hole transporting layer; 200 Å the complex doped (7%) CBP as the emitting layer; 100 Å of BCP (2,9-dimethyl-4,7-diphenyl-1,10-phenanthroline) as a hole and exciton blocking layer (HBL); 650 Å of Alq_3 (*tris*(8-quinolinato)aluminium) as electron transport layer; and a cathode composed of 10 Å lithium fluoride and 2000 Å aluminum were sequentially deposited onto the substrate to give the device structure. Fig. 1(a) and (b) show the multilayer structure of the device and the chemical structures of the molecules used in fabricating the EL device, respectively. The current–voltage (*I–V*) profiles and light intensity characteristics for the above-fabricated devices were measured in a vacuum chamber of 10^{-6} torr at ambient temperature using a Keithley 2400 Source Meter/2000 Multimeter coupled to a PR 650 Optical Meter.

3. Results and discussion

3.1. Syntheses and characterizations

The synthetic routes for the platinum(II) complexes described here involves two steps. In the first step, K_2PtCl_4 is reacted with an excess of bt/substituted bt to produce a chloride-bridged dinuclear complex (Fig. 2, inset), i.e. (bt/X-bt)Pt(μ-Cl)$_2$Pt(bt/X-bt). All these complexes, except (MeO-bt)Pt(μ-Cl)$_2$Pt(MeO-bt), are almost insoluble in common organic solvents which makes them impossible for solution phase characterization. The polar methoxy substituent is assumed to be responsible for making the corresponding dinuclear platinum(II) complex have a better solubility in more or less polar organic solvents. The ^{1}H NMR spectrum

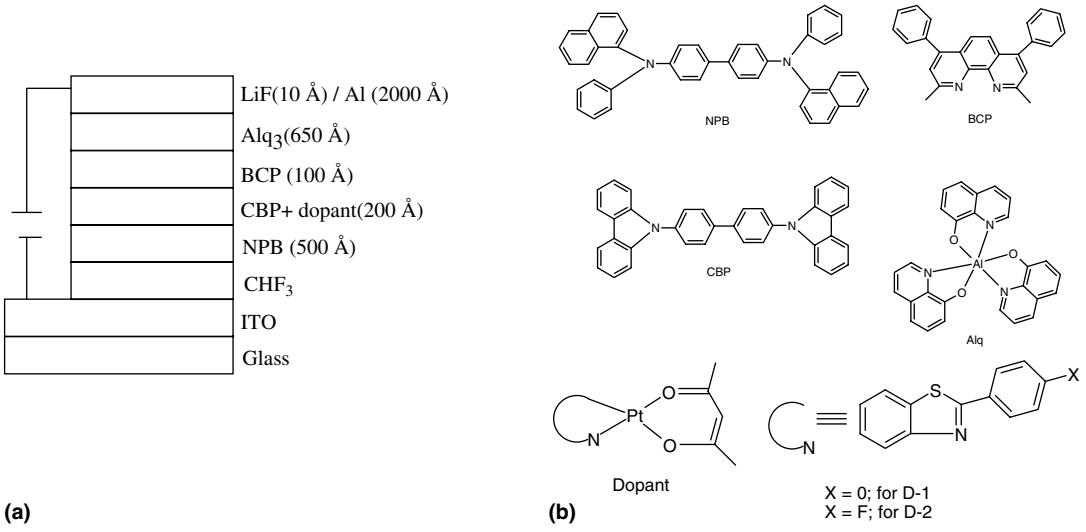

Fig. 1. (a) Multilayer device structure. (b) The chemical structures of the molecules used in this device.

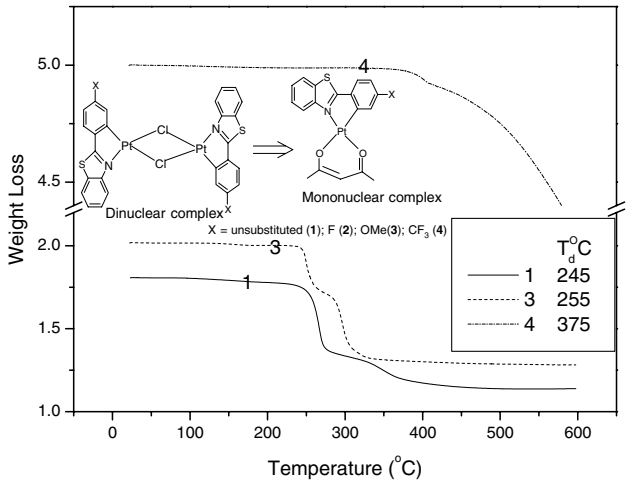

Fig. 2. TGA thermograms of the platinum(II) complexes **1**, **3** and **4**, T_d represents decomposition temperature (inset: the chemical structures of the complexes investigated).

of (MeO-bt)Pt(μ-Cl)$_2$Pt(MeO-bt) (deposited) shows the splitting of the methyl proton in the methoxy substituent of the dinuclear complex, suggesting that the two non-equivalent methoxy protons exist in the two separate ligands of that complex. It is the result from different interactions with the solvent molecules. The chloride-bridged dinuclear complexes can be readily dissociated to emissive, mononuclear complexes by replacing the bridging chlorides with monoanionic 2,4-pentanedionate (Fig. 2, inset). These mononuclear complexes were characterised by ^{1}H NMR spectra and elemental analyses, but ^{13}C NMR spectra were not recorded due to not having the required level of solubility in deuterated solvents. Thermogravitometric analysis (TGA) shows the stability of these complexes in the range of 245–375 °C (Fig. 2) and they can be easily sublimed at low pressure (10^{-3} mmHg).

3.2. Crystal structures

X-ray single crystal structure analysis was carried out for one of the platinum complexes **3**, which authenticates the square planar geometry (discrepancy factor ~5%; Fig. 3(a)). X-ray quality single crystals of the complex were grown by slow diffusion of methanol into a dichloromethane solution of **3**. The bond length of Pt1–N1 (2.02 Å) is slightly larger compared to that of common Pt–N bonds, as this N is opposite to the acetylacetonate oxygen atom, having a weak *trans* influence. The bond length of Pt1–O2 (2.085 Å) is higher compared to that of Pt1–O1 (1.994 Å), as O2 is *trans* to carbon which has a strong *trans*-influence. The bond length of Pt1–C9 (1.967 Å) is consistent with other reported cyclometallated complexes [6d,16]. The Pt(1)–O(1) (1.994 Å) and Pt(1)–O(2) (2.085 Å) bond lengths are also consistent with other reported cyclometallated–diketonato derivatives [17]. The C(9)–Pt(1)–O(1), 90.65(16)°; C(9)–Pt(1)–N(1), 80.48(17)°; O(1)–Pt(1)–N(1), 171.11(15)°; C(9)–Pt(1)–O(2), 176.82(15)°; O(1)–Pt(1)–O(2), 91.23(13)°; N(1)–Pt(1)–O(2), 97.62(14)° bond angles are typical for cyclometallates and –diketonate derivatives of Pt [16,17]. There is very little distortion away from the square plane. The molecular packing diagram of Pt(MeObt)(acac) (Fig. 3(b)) shows the molecules pack as head-to-tail dimers; each molecule of the dimer is related to the other by a center of inversion. The short inter plane and metal–metal distances (Pt1···Pt1 = 3.369; Pt2···Pt2 = 3.369; Plane–Plane = 3.360 Å;

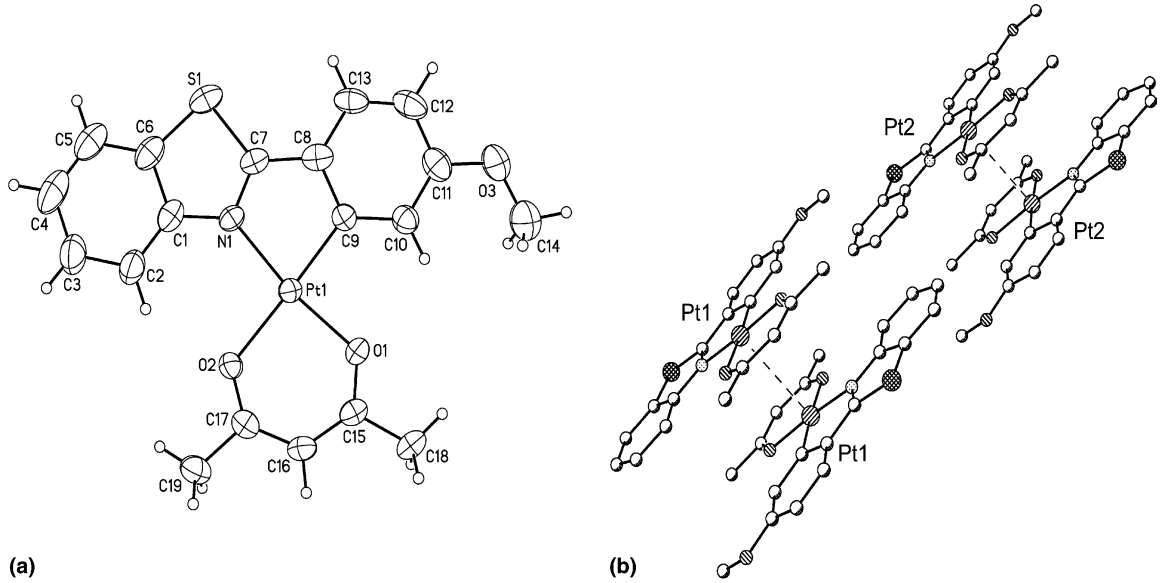

Fig. 3. (a) Molecular structure of complex **3** (shows 50% thermal probability); (b) molecular packing diagram showing the π stacking of complex **3**.

centre of symmetry is formed between the acac and the five membered ring) suggest that there exist extensive π–π and metal–metal interactions [6d] which support the excimer formation.

3.3. Photophysical behavior

The absorption spectra of all the complexes in dichloromethane were recorded at room temperature, and show intense higher energy transitions $^1\pi$–π^* (280–350 nm; $\varepsilon \sim 5 \times 10^3$ dm^3 mol^{-1} cm^{-1}) as well as comparatively lower energy, broad triplet state transitions (350–475 nm; $\varepsilon \sim 2 \times 10^3$ dm^3 mol^{-1} cm^{-1}), as shown in Fig. 4. These broad MLCT states exhibit solvatochromic effects. The complexes emit orange light in the solid state as well as in solution. Highly structured PL emission and sharp vibronic progressions of ~2185 cm^{-1} were observed (Fig. 5). These observations helped us to identify the nature of the lowest-emitting states of both triplet π–π* and MLCT character. In general, the electron-donating substituent raises the highest occupied molecular orbitals (HOMO) and the lowest unoccupied molecular orbitals (LUMO) and the reverse is truth for an electron-withdrawing substituent [18,19]. The complex **4** which contains electron-withdrawing substituted (–CF_3) benzothiazolate shows a bathochromic shifted emission, while those contain electron-releasing substituted (–F (**2**), –MeO (**3**)) benzothiazolates undergo *ipso*-chromic shifted emission with respect to the unsubstituted complex, **1**, as shown in Fig. 5. Hence it can be inferred that the position occupied by the substituents in (2-phenyl)-benzothiazolate of the iridium(III) complexes are dominated by LUMO character. The maximum absorbance and emission of all the complexes are listed in Table 1. The excimer formation was evidenced through the time resolved photoluminescence measurements [20]. The emission kinetic trace for one of the complexes **4** produced by excitation at 378 nm and monitored near the lower energy shoulder emission (e.g., 656 nm; Fig. 5) shows monoexponential decay behavior. The reciprocal of the lifetimes (known as emission decay rate constant, k_{obs}) obtained are shown in Fig. 6 as a function of concentration. The lifetime was found to decrease steadily with increasing concentration, indicative of excimer formation. The emission lifetime of the monomer of complex **4** at infinite dilution, τ_0 (0.58 μs), and the apparent rate constant of self-quenching, k_Q, were determined by using Eq. (1) (0.58 μs; 7×10^8 M^{-1} s^{-1}) from the linear variation of the observed emission decay constant, k_{obs}, as a function of the concentration of the complex, [Pt]. The high value of k_Q indicates extensive excimer formation. It should also be true for the other platinum(II) complexes.

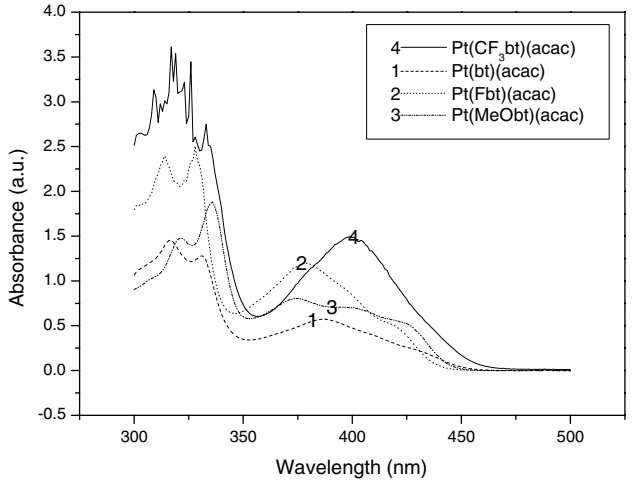

Fig. 4. UV–Vis absorption spectra of the complexes **1**, **2**, **3** and **4** measured at 298 K showing the tuning of the lowest excited state.

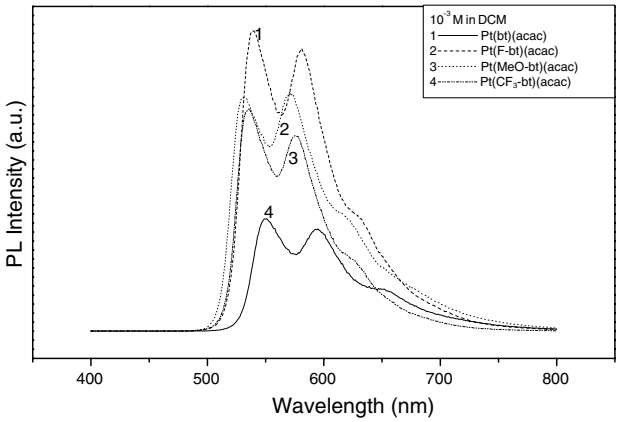

Fig. 5. PL spectra showing tuning of emission wavelength with respect to the electronic properties of the substituents.

$$k_{obs} = 1/\tau_0 + k_Q[Pt]\ [20] \quad (1)$$

Table 1
Absorption and emission properties of the platinum(II) complexes **1**–**4**

Complexes	abs, λ_{max}, nm (logε)[a]	Emission at 298 K, λ_{max}, nm[a]
1	228 (6.0); 254 (5.9); 262 (5.7); 316 (5.8); 330 (5.7); 387 (5.4); 431 (5.0)	539; 580
2	228 (5.8); 252 (5.7); 313 (5.6)sh; 327 (5.6); 377 (5.3)sh; 416 (5.0)	531; 571
3	228 (6.2); 242 (6.1)sh; 279 (5.9); 320 (6.1); 334 (6.1); 373 (5.7); 402 (5.6)sh; 423 (5.5)sh	534; 575
4	228 (6.2); 259 (6.2); 318 (6.1); 333 (6.0)sh; 398 (5.7)b	551; 594

[a] In dichloromethane; sh, shoulder; b, broad.

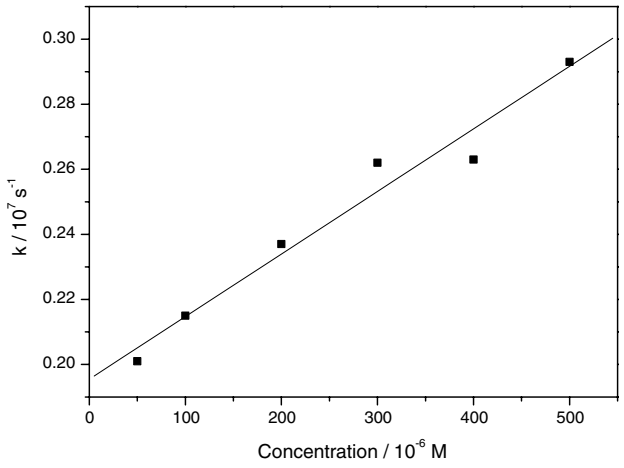

Fig. 6. Plot of the measured luminescence decay constants versus concentration of platinum complex **4**.

3.4. Electroluminescence

All these complexes are thermally stable up to 245–375 °C and they can be easily sublimed at low pressure (10^{-3} mmHg) and emit tunable bright yellow-orange light at room temperature. All these features make them good emitters in highly efficient EL devices. The platinum complexes, **1** and **2** (the corresponding devices denoted as D-1 and D-2, respectively) were doped into the host material, CBP (4,4′-(*N*,*N*′-dicarbazole)biphenyl), in the emitting zone with doping contents of 5%, 7% and 9%. The observed device performances were found to vary marginally throughout the doping concentration range (Table 2). Current-density, voltage and luminance characteristics (*I*–*V*–*L*) for devices D-1 and D-2 with 5% doping level are shown in Fig. 7(a) and (b), respectively. Comparison of device performances for the devices D-1 and D-2 at 5% doping level are also summarized in Table 3, which show the maximum luminance yields of 14.3 and 16.0 cd A^{-1} @2 mA cm^{-2} for D-1 and D-2, respectively. The maximum emission wavelength (λ_{em}^{max}) for D-2 shows apparent *ipso*-chromic shift with respect to that of device D-1 (Fig. 8), as observed in PL emission spectra. The maximum emission wavelengths in the EL spectra are found to be independent of the applied voltage (for current density up to 100 mA cm^{-2}), but show bathochromically shifted emission with increasing doping concentration. The EL intensity of the shoulder peak

Table 2
EL performance of D-1 and D-2 at different dopant concentrations [at 20 mA cm^{-2} current density in parentheses]

Device	wt%	V_d (V)	L_{max} (cd m^{-2})	CIE		$\eta_{ext.\ max}$ (%)	$\eta_{L,\ max}$ (cd A^{-1})	$\eta_{P,\ max}$ (lm W^{-1})
				x	*y*			
D-1	5	10.7	2573	0.48	0.50	4.9	12.9	3.8
	7	11.2	2638	0.49	0.48	5.6	13.2	3.7
	9	10.6	2197	0.52	0.47	5.3	11.0	3.3
D-2	5	11.2	2820	0.47	0.50	5.7	14.1	4.0
	7	11.5	2769	0.48	0.58	6.9	13.8	3.8
	9	11.7	2442	0.47	0.58	6.7	12.2	3.3

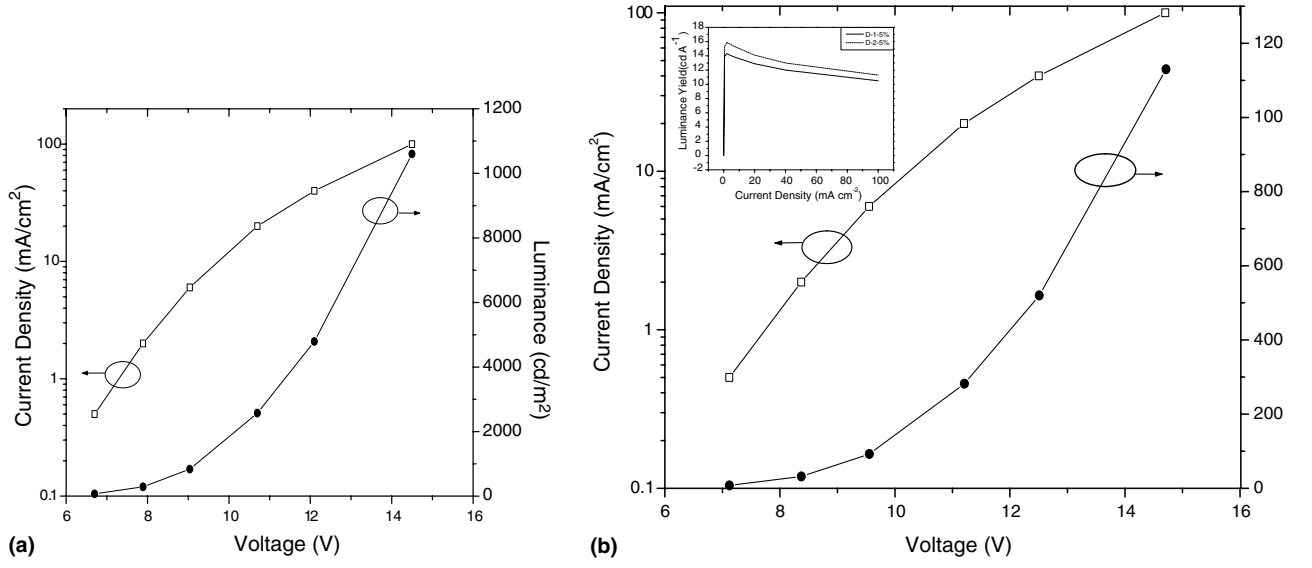

Fig. 7. Current density, voltage and luminance characteristics for OLED using complexes **1** (a) and **2** (b) with 5% doping level (b: inset: plot of luminescence efficiency vs. current density).

Table 3
Comparison of EL performances for D-1 and D-2 with 5% doping level operated at different current densities

Current density (mA cm^{-2})	V (V)		L (cd m^{-2})		CIE				η_{ext} (%)		η_L (cd A^{-1})		η_P (lm W^{-1})	
					x	y	x	y						
	D-1	D-2	D-1	D-2	D-1		D-2		D-1	D-2	D-1	D-2	D-1	D-2
0.5	6.7	7.1	70	77	0.40	0.50	0.49	0.50	5.4	6.5	13.9	15.3	6.5	6.5
2.0	7.9	8.4	286	319	0.49	0.50	0.48	0.51	5.5	6.6	14.3	16.0	5.7	6.6
6.0	9.0	9.6	834	924	0.49	0.50	0.48	0.51	5.3	6.3	13.9	14.8	4.8	6.3
20.0	10.7	11.2	2573	2820	0.48	0.50	0.48	0.51	4.9	5.7	12.9	14.1	3.8	5.7
40.0	12.1	12.5	4787	5197	0.48	0.50	0.48	0.51	4.6	5.3	12.0	13.0	3.1	5.3
100.0	14.5	14.7	10550	11320	0.48	0.50	0.47	0.51	4.0	4.6	10.6	11.3	2.3	4.6

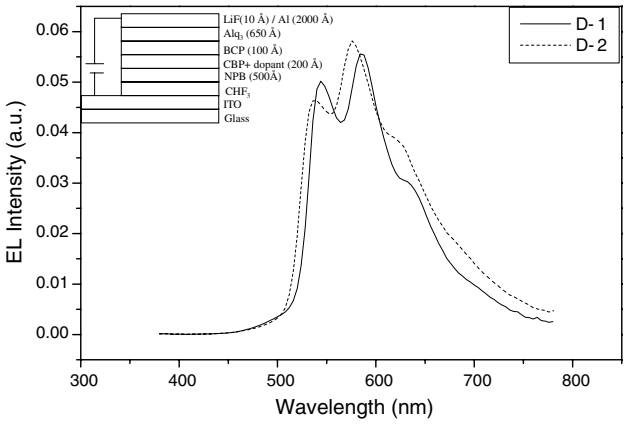

Fig. 8. EL spectra for the platinum(II) complexes **1** and **2** (inset: multilayer EL device configuration).

(~625–630 nm) has been observed to increase with increasing doping concentration, whereas that of the other two major peaks was found to decrease (~540 and ~584 nm). These observations support that the emission from the shoulder peak is generated from the excimer and it is also consistent with the results obtained from the molecular packing diagram (Fig. 3(b)) and concentration dependent luminescence decay measurements discussed before. It is to be noted that at 100 mA cm^{-2} current density, the luminances are found to be 10550 and 11320 cd m^{-2}, obtained for D-1 and D-2, respectively, and under similar conditions there have not been significant changes of luminance yields (i.e., 10.6 and 11.3 cd A^{-1}, for D-1 and D-2, respectively).

4. Conclusion

The syntheses and characterizations of a series of platinum(II) complex dopants have been performed. The EL performances of OLEDs employing these platinum(II) dopants are found to be substantially superior to those previously reported for OLEDs based on cyclometallated platinum(II) complexes [6]. These EL results were even far better than those previously reported [21] where a similar type of cyclometallated iridium(III) dopants were used in the same device structure. It should be mentioned that the device containing fluoro-substituted dopant shows relatively better EL performances with respect to that using the unsubstituted benzothiazolato Pt(II) complex.

Acknowledgements

The work has been supported in part by the Program for Promoting University Academic Excellence from Ministry of Education, Taiwan, ROC under the Contract No. 91-E-FA04-2-4 (B).

Appendix A. Supplementary data

Crystallographic data for the structural analysis have been deposited with the Cambridge Crystallographic Data Centre, CCDC No. 247375 for compound Pt(MeO-bt)(acac). Copies of this information may be obtained free of charge from the Director, CCDC, 12 Union Road, Cambridge, CB2 1EZ, UK (fax: +44 1223 336033; email: deposit@ccdc.cam.ac.uk or http://www.ccdc.cam.ac.uk). Supplementary data associated with this article can be found, in the online version at doi:10.1016/j.poly.2005.02.009.

References

[1] (a) V. Balzani, A. Credi, F. Scandola, L. Fabbrizzi, A. Poggi (Eds.), Transition Metals in Supramolecular Chemistry, Kluwer, Dordrecht, The Netherlands, 1994;
(b) J.M. Lehn, Supramolecular chemistry-concepts and perpectives, VCH, Weinheim, Germany, 1995;
(c) C.A. Bignozzi, J.R. Schoonover, F. Scandola, Prog. Inorg. Chem. 44 (1997) 1.
[2] (a) F.G. Gao, A.J. Bard, J. Am. Chem. Soc. 122 (2000) 7426;
(b) M. Grätzel, Nature 414 (2001) 338;
(c) C.F. Chow, B.K.W. Chiu, M.H.W. Lam, W.Y. Wong, J. Am. Chem. Soc. 125 (2003) 7802.
[3] (a) J. Breu, C. Kratzer, H. Yersin, J. Am. Chem. Soc. 122 (2000) 2548;
(b) B. Carlson, G.D. Phelan, W. Kaminsky, L. Dalton, X. Jiang, S. Liu, A.K.Y. Jen, J. Am. Chem. Soc. 124 (2002) 14162.

[4] (a) V.W.W. Yam, Chem. Commun. (2001) 789;
(b) K.K.W. Lo, W.K. Hui, D.C.M. Ng, J. Am. Chem. Soc. 124 (2002) 9344.
[5] (a) I.M. Dixon, J.P. Collin, J.P. Sauvage, L. Flamigni, S. Encinas, F. Barigelletti, Chem. Soc. Rev. (2000) 385;
(b) S. Lamansky, P. Djurovich, D. Murphy, F. Abdel-Razzaq, H.E. Lee, C. Adachi, P.E. Burrow, S.R. Forrest, M.E. Thompson, J. Am. Chem. Soc. 123 (2001) 4304;
(c) Md.K. Nazeeruddin, R. Humphry-Baker, D. Berner, S. Rivier, L. Zuppiroli, M. Graetzel, J. Am. Chem. Soc. 125 (2003) 8790;
(d) W.J. Finkenzeller, H. Yersin, Chem. Phys. Lett. 377 (2003) 299;
(e) P. Coppo, E.A. Plummer, L. De Cola, Chem. Commun. (2004) 1774.
[6] (a) M.A. Baldo, d.F. O'Brien, Y. You, A. Shoustikov, S. Sibley, M.E. Thompson, S.R. Forrest, Nature 395 (1998) 151;
(b) R.C. Kwong, S. sibley, T. Dubovoy, M.A. Baldo, S.R. Forrest, M.E. Thompson, Chem. Mater. 11 (1999) 3709;
(c) V. Cleave, G. Yahioglu, P.L. Barny, R.H. Friend, N. Tessler, Adv. Mater. 11 (1999) 285;
(d) J. Brooks, Y. Babayan, S. Lamansky, P.I. Djurovich, I. Tsyba, R. Bau, M.E. Thompson, Inorg. Chem. 41 (2002) 3055.
[7] F. Barigelletti, D. Sandrini, M. Maestri, V. Balzani, A. von Zelewsky, L. Chassot, P. Jolliet, U. Maeder, Inorg. Chem. 27 (1988) 3644.
[8] T.K. Aldridge, E.M. Stacy, D.R. Mcmillin, Inorg. Chem. 33 (1994) 722.
[9] J.M. Bevilacqua, R. Eisenberg, Inorg. Chem. 33 (1994) 2913.
[10] C. Che, S. Chan, H. Xiang, M.C.W. Chan, Y. Liu, Y. Wang, Chem. Commun. (2004) 1484.
[11] G.M. Sheldrick, SAINT; Bruker Analytical X-ray Instrument Division; Madison, WI, 1998.
[12] G.M. Sheldrick, SHELXTL, version 5.1; Bruker AXS GmbH, Karlsruhe, Germany, 1998.
[13] A. Brembilla, D. Roizard, P. Lochon, Synth. Commun. 20 (1990) 3379.
[14] G.W.V. Cave, F.P. Fanizzi, R.J. Deeth, W. Errington, J.P. Rourke, Organometallics 19 (2000) 1355.
[15] S. Lamansky, M.E. Thompson, V. Adamovich, P.I. Djurovich, C. Adachi, M.A. Baldo, S.R. Forrest, R. Kwong, US patent, 0182441 A1, 2002.
[16] J. Breu, K.J. Range, A. von Zelewsky, H. Yersin, Acta Crystallogr. C 53 (1997) 562.
[17] M. Ghedini, D. Pucci, A. Crispini, G. Barberio, G. Barberio, Organometallics 18 (1999) 2116.
[18] R. Pohl, J. Pavel Anzenbacher, Org. Lett. 5 (2002) 2769.
[19] R. Pohl, V.A. Montes, J. Shinar, J. Pavel Anzenbacher, J. Org. Chem. 69 (2004) 1723.
[20] J.A. Williams, A. Beeby, E. Stephen Davies, J.A. Weinstein, C. Wilson, Inorg. Chem. 42 (2003) 8609.
[21] I.R. Laskar, T.-M. Chen, Chem. Mater. 16 (2004) 111.